frontiers | Frontiers in Communications and Networks

ORIGINAL RESEARCH
published: 27 April 2022
doi: 10.3389/frcmn.2022.867045

Smart Self-Coherent Optical Communication for Short Distances

Pantea Nadimi Goki[1]*, *Muhammad Imran*[1], *Fabio Cavaliere*[2] and *Luca Potì*[3,4]

[1]TeCIP Institute, Scuola Superiore Sant'Anna, Pisa, Italy, [2]Ericsson Italy, Pisa, Italy, [3]CNIT, Photonic Networks and Technologies National Laboratory, Pisa, Italy, [4]Università Mercatorum, Rome, Italy

We proposed and investigated a high-performance, energy-efficient, and low-cost self-homodyne coherent detection transmission (SHCDT) system for the 5G access network segment assuring high capacity and light digital signal processing (DSP) at the same time, avoiding the local oscillator for detection. The system implementation is based on a code-based spectral shaping at the transmitter and carrier extractor at the receiver. In the self-homodyne coherent system, a continuous wave carrier is transmitted together with the modulated signal. After transmission, at the receiver, the carrier is extracted and used as a local oscillator (LO) to prevent frequency offset with respect to the transmitted signal and phase noise, resulting in a decrease in the digital signal processing (DSP) complexity. Transmission results indicate that even a low portion of the residual local oscillator (LO) on the transmitted signal at the receiver side can lead to an increase in the signal-to-noise ratio (OSNR) penalty. Consequently, applying a proper technique to separate the unmodulated carrier and the modulated signal is the key to the system's performance. We evaluated the self-homodyne coherent system performance through numerical analysis and experimental validation. The performance of the proposed self-coherent system, using a narrow bandwidth Fabry–Perot filter for optical carrier extraction, is evaluated experimentally on a 28 Gbaud dual-polarization 16QAM transmission system considering different code block lengths for signal spectral shaping through bit-error-rate (BER) measurements.

Keywords: coherent Detection, polarization Control, short-reach communication, spectral shaping, laser phase noise, low Cost

OPEN ACCESS

Edited by:
Xian Zhou,
University of Science and Technology Beijing, China

Reviewed by:
Lu Zhang,
Zhejiang University, China
Yuyuan Gao,
University of Science and Technology Beijing, China

***Correspondence:**
Pantea Nadimi Goki
pantea.nadimigoki@santannapisa.it

Specialty section:
This article was submitted to Optical Communications and Networks, a section of the journal Frontiers in Communications and Networks

Received: *31 January 2022*
Accepted: *25 March 2022*
Published: *27 April 2022*

Citation:
Nadimi Goki P, Imran M, Cavaliere F and Potì L (2022) Smart Self-Coherent Optical Communication for Short Distances. Front. Comms. Net 3:867045. doi: 10.3389/frcmn.2022.867045

1 INTRODUCTION

In the overwhelming majority of current optical transport networks, transmission at 100 Gbit/s is performed using dual-polarization QPSK coherent optical interfaces. Capacity enhancement at 400 Gbit/s is possible by using 16QAM instead of QPSK and doubling the device's bandwidth from 25 to 50 GHz. Standards for interoperable 100 and 400 Gbit/s optical interfaces operating over metro distances are specified by ITU-T G.8300 (ITU 2020) and G.6982 Recommendation (ITU 2019), respectively. Compared to intensity-modulated direct-detection systems (IM-DD), where information data are mapped onto amplitude levels of an optical signal, coherent systems transmit and detect information on both signal amplitude and phase. Due to the one-dimensional modulation, the spectral efficiency (SE) of the IM-DD system is significantly limited; therefore, it cannot reach beyond 100 Gb/s (Che et al., 2014), (Che and Shieh, 2016). In the coherent system's transition, two-dimensional modulation (or higher) will be performed (Morsy-Osman and Plant, 2018). This has the twofold advantage of allowing the use of complex modulation

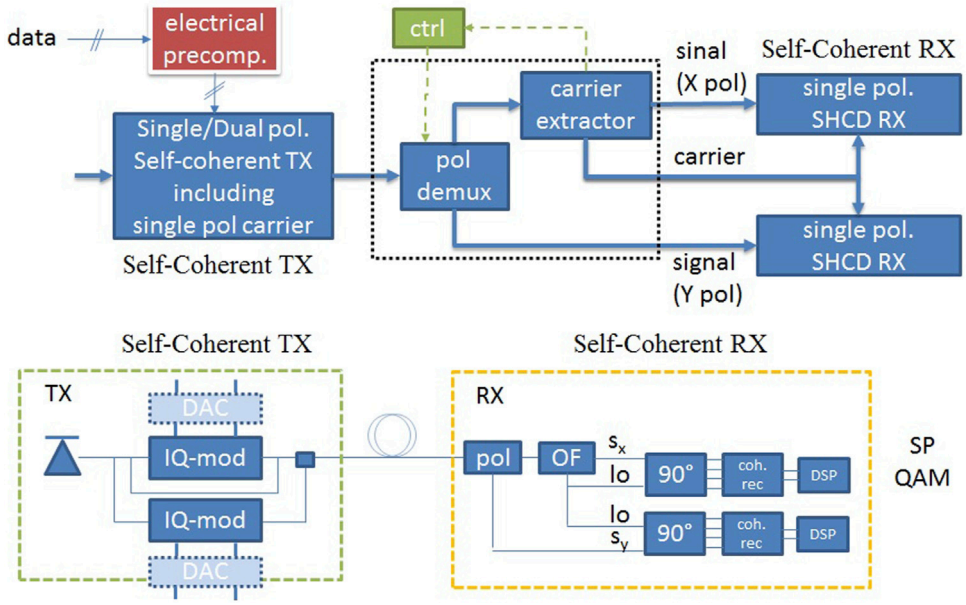

FIGURE 1 | Self-coherent system architecture.

schemes, such as QAM, increasing the system's capacity and the use of equalization techniques for recovering propagation impairments such as fiber chromatic dispersion. The latter feature led to big saving in network costs, avoiding the use of dispersion compensating fiber (and double stage optical amplifiers to host it) in the optical link. The absence of the dispersion compensating fiber greatly simplified system design rules (in old systems, dimensioning position and size of the compensating modules were crucial for optimizing the system performance), positively impacting operational cost. Although coherent optical transmission was proposed decades ago, it could be deployed only after the miniaturization and the integration of electronic circuits, which made it possible to implement complex processing functions in small integrated circuits, with acceptable power consumption (a few tens of watts). Photonics followed a similar path toward higher integration, though with considerable delay: the number of functions that can be integrated into a photonic chip is an order of magnitude less than the functions in an electronic chip of the same size. Moreover, the optical processing functions are mostly analog, reducing the processing possibilities compared with electronic processing. However, combining photonic and electronic processing in the same system can enable new architectures with improved cost and power consumption. The success of coherent optical transmission in metro and long-haul optical networks (spanning from hundreds to thousands of km) could not be replicated in shorter-distance radio and fixed-access networks (Alimi et al., 2021) which are more cost-sensitive. Energy efficiency is another issue: the integrated circuits used for signal postprocessing in a coherent receiver consume tens of watts, while a few watts would be acceptable. On the other hand, the capacity required by modern radio access networks can easily achieve hundreds of Gbit/s, making coherent transmission an appealing technique, despite cost and power consumption issues. Coherent optical systems at the receiver use a CW laser as a local oscillator. The local oscillator light is coupled to the received signal. If the local oscillator frequency is not equal to the transmitted optical carrier, a frequency offset appears (some GHz in practical systems) that must be compensated for at the receiver, causing an increase in DSP complexity. Furthermore, the local oscillator phase noise is transferred onto the signal, and mitigating it requires expensive narrow-linewidth lasers to be used as the local oscillator.

In coherent systems, chromatic dispersion compensation is implemented by DSP at the receiver, which leads to indisputable benefits in long haul systems. However, in access networks, where the distances are much shorter, pre-compensation techniques may be considered as energy-efficient alternatives. Transmission of two orthogonal polarization in the coherent systems requires a front-end coherent receiver with a 90° hybrid device. Otherwise, a polarization controller Sacher et al. (2014), Sorianello et al. (2016) at the receiver must be applied, to rotate the polarization of the local oscillator, aligning it to the received signal. A self-homodyne coherent system can be considered a cost-effective and energy-efficient option (Adhikari et al., 2011). In the studies by Che et al. (2013) and Chen et al. (2014), a self-homodyne system was reported based on a temporal signal-carrier interleaving (SCI) scheme, resulting in increasing the DSP complexity. The LO transmits so that the CW tone occupies one-third of the time-domain waveform. At the receiver, the waveform is split into two copies, which are delayed relative to each other by t0 for self-coherent detection *via* a 90-degree hybrid. A self-homodyne system for short-reach transmission was proposed by Sowailem et al. (2016), based on the concept of transmitting

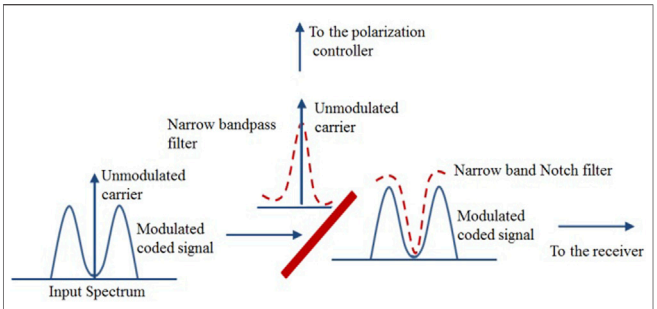

FIGURE 2 | Operation principle of the carrier extractor.

the LO from the transmitter to the receiver over a separate fiber for two polarization transmission or with the same fiber but over the other polarization of signal for one polarization transmission system. In this article, we propose a novel self-coherent system based on the concept of transmitting the LO from the transmitter to the receiver, along with one polarization over the same fiber in the two-polarization transmission system. In this system, the polarization recovery at the receiver input was omitted. The validation of the proposed system was carried out through numerical simulation and experimental measurements. One of the benefits of the proposed system is that the DSP for both frequency offset compensation and phase noise transmission mitigation can be removed, resulting in reduction for DSP complexity.

This article is organized as follows: the proposed system is introduced in **Section 2**. The system design and analysis are discussed from a conceptual point of view. In **Section 3**, the numerical and experimental validation is demonstrated, and the results are reported. The last section provides a brief discussion on the advantages of the proposed system.

2 MATERIALS AND METHODS

2.1 Self-Homodyne Coherent Detection Transmission System

This research activity is focused on the self-coherent optical system demonstration for the access network segment, promising high capacity and low DSP complexity concurrently. Such a solution includes system aspects, integrated devices, and dedicated DSP implementation. This section defines the core essence of the proposed system.

2.2 System Design and Analysis

In conventional self-coherent systems, a CW laser, also known as a local oscillator (LO), is essential at the receiver to recover the transmitted signal. In this research, we proposed a self-coherent system that is free of CW requirements in the receiver for recovering the transmitted signal. In the SHCDT system, the fundamental aspect is in transmitting an unmodulated CW laser with one polarization of the modulated signal and using it as an LO at the receiver. This method prevents the frequency offset and phase noise transfer from the LO to the received signal. Consequently, receiver DSP does not require recovery of the frequency offset between the local oscillator and transmitted optical carrier, leading to decreasing DSP complexity. While in regular self-coherent systems, mitigating the phase noise transmission requires expensive narrow-linewidth lasers to be used as a local oscillator, and the proposed SHCDT system assures detection devoid of phase noise transmission. Generally, in practical self-coherent systems, a frequency offset of the order of a few GHz or less must be compensated, while in the proposed system, the local oscillator frequency is equal to the transmitted optical carrier frequency, and the beating term generated by photodetection is proportional to the modulated signal.

2.3 Detailed Description System Configuration

Figure 1 illustrates the scheme of the proposed system. A high-output tunable CW laser, as a light source, is connected to a dual (or single) polarization IQ modulator. In this scheme, data are sent over two linear orthogonal polarization states to double the bit rate of the transmitted signal. The unmodulated optical carrier is transmitted on one of the two polarizations (e.g., pol X) *via* the coupling after the modulator. The chromatic dispersion is pre-compensated, optically or electrically, at the transmitter side *via* a digital-to-analog converter (DAC). In standard coherent systems, chromatic dispersion is compensated by means of FFT and digital filtering inside the receiver DSP. However, SHCDT has been considered a transmission solution for short distances, so a pre-compensation technique can be easily implemented. That would be considered an energy-efficient alternative. At the receiver side, the signal polarization arrives rotated at a random angle regarding the transmitted polarization. At the receiver, a polarization demultiplexer (P-DeMux) rotates the polarization of the dual-polarization signal so that the two orthogonal polarization states are separated and individually sent to their two outputs. A possible implementation is shown in a study by Sacher et al. (2014). After the P-DeMux, X polarization is sent into the carrier extractor, and the other polarization (pol Y) is sent to the single-polarization self-coherent receiver. Then, the optical carrier is extracted, exploiting a 2-port tunable optical filter (such as microring-resonator-based filters). Typically, the first port of the carrier extractor acts as a tunable narrow bandpass filter that rejects the modulated signal and only keeps the unmodulated carrier. A second port of the carrier extractor performs the inverse operation, acting as a notch filter, that is, rejecting the carrier and extracting the modulated signal. The operation of the carrier extractor is demonstrated in **Figure 2**. The effect of the residual signal on the extracted carrier is an important issue that must be considered. A proper technique must be used on the receiver side, obtaining the extracted carrier with the minimum residual signal. An appropriate method to mitigate the residual signal is to couple the carrier to a modulated signal whose spectral shape has been modified before transmission and then extract the carrier at the receiver side using a narrow bandwidth filter. The signal spectral shape has been modified in such a way that the power of the

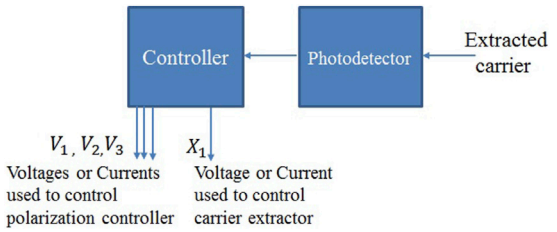

FIGURE 3 | Input and output variables of the controllers.

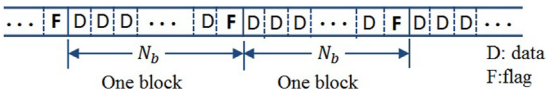

FIGURE 4 | Binary block codes (BBC) description.

modulated signal is low within the band of the filter. This method leads to minimizing the value of the residual signal on the extracted carrier. Performing this modification is possible by using coding techniques (such as Manchester) that deplete the signal spectrum around the DC component.

In a standard self-coherent system, the two polarization states remain orthogonal and randomly rotated during propagation. At the front-end of a standard coherent receiver, the local oscillator and signal are mixed in a so-called 90° hybrid device, placed before the photodiode (dual-polarization receiver). Alternatively, a polarization controller Sacher et al. (2014), Sorianello et al. (2016) may be used to rotate the polarization of the local oscillator, aligning it to the received signal. After photodetection, the data sent over the two polarizations are recovered utilizing the electrical equalizer. In the proposed system, the transmitted optical carrier is used as the local oscillator, so its angle with the received signal is known and no polarization recovery is needed. However, if integrated photonic circuits are used at the receiver front-end, polarization alignment is needed anyway because photonic integrated circuits usually accept only a single-input linear polarization state. Active polarization alignment is feasible with silicon photonics devices. An example is reported by Sorianello et al. (2016), based on phase shifters in optical interferometers. Any polarization rotation scheme requires an iterative process to converge using as a control variable a performance parameter detected at the receiver (e.g., BER or power on each polarization) or some signal characteristics used to distinguish the two transmitted polarization states (e.g., different pilot tone frequencies for the two polarizations). Issues in convergence speed and outage probability can have several causes. For example, the control variable may be affected by noise or measurement inaccuracy, or the transducers that convert the electrical control variable (a voltage or a current) into the optical parameter to control (e.g., a phase shift) may have a limited dynamic range and bandwidth. Having a common controller for carrier extractor and polarization controller helps fast convergence and mitigates outage issues. The input and output variables of the controller are shown in **Figure 3**. The controller iteratively sets the voltages (or the currents) used by the polarization controller. In a typical configuration, they could be three voltages, V1, V2, and V3, that control the phase shifts in the arms of consecutive Mach Zehnder interferometers (MZ) (Sorianello et al., 2016). The current (or the voltage), X1, is used to control the central frequency of notch and passband filters in the carrier extractor until the photo-detected current Iin, proportional to the carrier optical power, is maximized. Widespread algorithms (e.g., steepest descent and gradient algorithm) can be used for this purpose.

2.4 Code Definition and Implementation

Various codes have been investigated; among all, a set of codes called binary block codes (BBCs), which have been extensively used for DC suppression Greenstein (1974), Cavers and Marchetto (1992), provided a perfect spectral shaping with low signal power around the DC component. Appling BBC on a bitstream introduces a flag "*F*" bit at the end of each block of length N_b-1, as is illustrated in **Figure 4**. Block length N_b providing code transmission efficiency is calculated as follows:

$$\eta_b = \frac{(N_b - 1)}{N_b}, \tag{1}$$

and a net rate (R) where the gross rate is RG is calculated as follows:

$$R = \eta_b \, . \, R_G, \tag{2}$$

Flag bit "*F*" can be easily calculated after definition of Running Interference Sum (RIS) and Running Digital Sum (RDS), given by

$$RIS(i) = \sum_{j=0}^{N_b-1} y(iN_b + j), \tag{3}$$

$$RDS(r) = \sum_{-\infty}^{r} F(i) RIS(i), \tag{4}$$

where

$$F(i) = \begin{cases} 1, & if\ RIS(i)RDS(i-1) \le 0 \\ -1, & otherwise. \end{cases}. \tag{5}$$

Considering a self-coherent system carrying RG = 224 Gb/s in a dual-polarization configuration, using BBC can lead to an error-free operation for both polarizations with a low net rate reduction.

The depletion around the DC component in the signal spectrum depends on the BBC block length. The different block length leads to various code efficiencies, which affect system performance. In our previous activity (Imran et al., 2021), we have shown that using long codes in a simple configuration (block length = 30 bits) results in a higher OSNR penalty than using the short codes (block length = 4 bits) at a BER of 10^{-4}.

The BBC has been developed and applied to four binary signals used for 16-QAM (I) and (Q) generation, and the results of using different BBC lengths are illustrated in **Figure 5**. As was expected, the BBC removes the DC

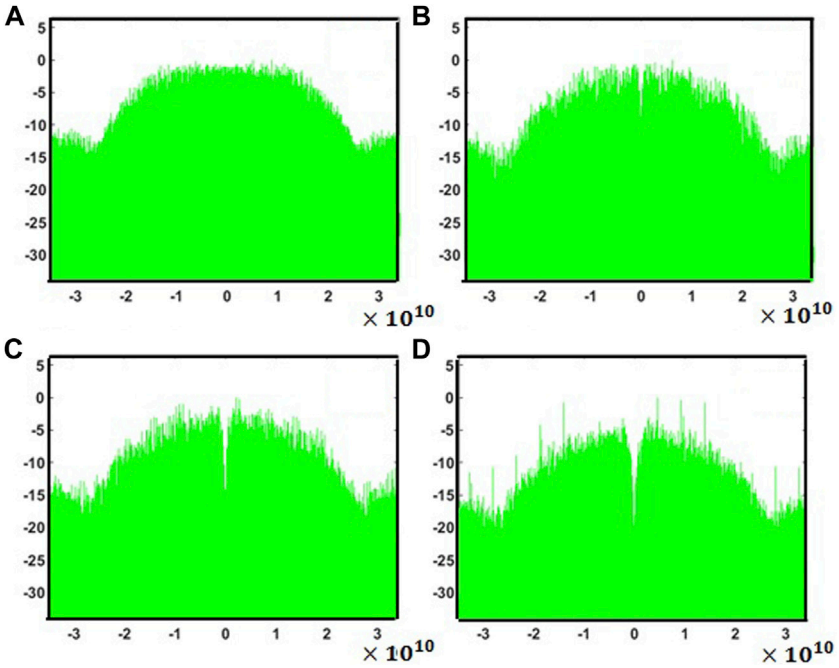

FIGURE 5 | Modulated signal spectra for different BBC efficiencies. **(A)** η_b = 1 (i.e., no BBC). **(B)** η_b = 9/10. **(C)** η_b = 7/10. **(D)** η_b = 5/10.

components. In addition, different code efficiencies result in different depletions. In practice, a notch appears in the spectrum, whose bandwidth is dependent on the coding efficiency. It must be noticed that for any fixed efficiency, notch bandwidth is fixed in terms of normalized frequency, that is, by increasing signal band rate, notch bandwidth will directly increase. This fact becomes very important when a filter is used to extract the carrier in the self-coherent scheme.

System performance varies with filter type, depth, and bandwidth on the receiver side. A proper investigation is needed to design the best integrated solution. This effect also can be mitigated by using spectral shaping at the transmitter through the coding technique.

2.5 Advantages of the Proposed System

The proposed self-coherent system presents several advantages. First, laser phase noise is mitigated at the receiver side due to self-coherent operation. Moreover, the receiver DSP does not require any recovery of frequency offset between the local oscillator and transmitted optical carrier. The optical front-end of the receiver is cost-effectively implemented in silicon photonics. Finally, the concurrent control on received signal polarization and optical carrier extraction mitigate the issues of current polarization controllers in terms of dynamic range and outage probability.

3 RESULTS

3.1 Performance Validation

We investigated the performance of the designed SHCDT system through numerical simulation and experimental measurements. The results of the simulated and measured system are reported in this section.

3.2 Numerical Investigation and Simulative Evaluation

A numerical investigation has been carried out based on the complete scheme, as shown in **Figure 1** so that one polarization (pol X) carries both signal and carrier, but the other is just the signal. First, we investigated code implementation on system performance. Afterward, to properly model the system, the numerical simulation was performed based on the parameters used in the experimental measurements.

3.2.1 BBC Performance

We evaluated the performance of BBC for the self-coherent implementation through simulation of a 28 Gbaud, 2-pol, 16_QAM-modulated signal with the power of −2.5 dBm and 2^{11}-1 pseudo-random bit sequence (PRBS) data. On the transmitter side, two polarizations were generated separately. We included a dual-polarization transmitter where data are independently generated for each polarization. The BBC was applied only on one polarization (X-pol). The (LO) carrier with power 14 dB higher than the signal was coupled with X-polarization. The Y-polarization did not include either the carrier or the BBC. On the receiver side, a single-polarization self-coherent receiver has been utilized. The two polarizations have been first received and processed individually. A 600-MHz-bandwidth Gaussian filter has been used for LO extraction from X-polarization. After photodetection, the data sent over the single polarization were recovered using the electrical

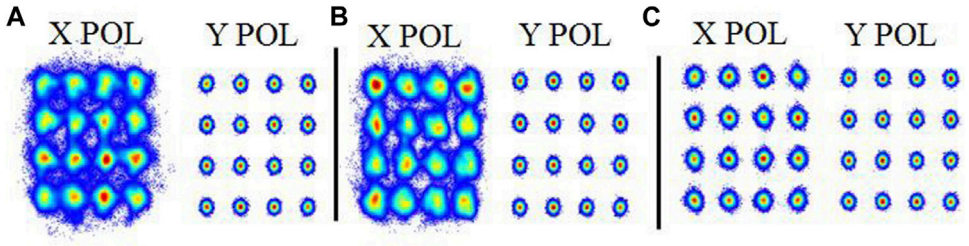

FIGURE 6 | Performance evaluation including X and Y received polarizations when only X-polarization is coded with the different BBC block length. The corresponding BER is **(A)** no BBC, X-pol BER = 6.3423e-02, and Y-pol BER = 3.0300e-06. **(B)** BBC length = 30 bits, X-pol BER = 1.4197e-02, and Y-pol BER = 0.00. **(C)** BBC length = 4 bits, X-pol BER 0.00, and Y-pol BER = 0.00.

equalizer (a single polarization standard butterfly equalizer used in optical communication). In subsequent analysis, system implementation in back-to-back configuration (B-to-B) was evaluated based on the BBC impact on system performance. Coded signal, with different lengths, provided zero BER at SNR = 28 dB. Accordingly, the BBC has no impact on the B-t-B transmission. **Figure 6** shows received constellations for both polarizations with evaluated BER values, when BBC is not used (a), and implemented over a length of 30 (b) and 4 (c) bits, while only X-polarization is coded. When the uncoded signal is transmitted, the performance implementation on X-polarization in terms of BER measurement is not good enough. The notch filter completely degrades the X-pol signal, and the transmitted information could not be recovered. On the other hand, using long codes (block length = 30) optimized the system performance, but it did not give an error-free operation. Finally, the best performance was provided using the short block length of the BBC (block length = 4).

Without BBC, X-polarization is mainly affected by a notch filter for carrier extraction, whereas Y-polarization is slightly perturbed by LO noise due to the extraction process, including the X-polarization signal (**Figure 6A**). When BBC is applied, the spectral shape of the signal is modified so that the signal spectrum around the DC component depletes and a hole appears in the signal spectrum, causing the LO extraction process to become less noisy. Therefore, the BER decreases for both received polarizations (**Figures 6B,C**). As is illustrated in **Figures 6B,C**, using long codes affects system performance, while short codes provide the best implementation of the system performance. In this simulation, the DSP unit at the Rx is similar to the DSP of a standard coherent system; however, the DSP complexity is reduced due to the absence of frequency offset and phase noise. Moreover, the receiver DSP does not require compensating for chromatic dispersion.

3.2.2 Transmission Simulation

The performance of the proposed system was further evaluated through simulation based on the actual system structure and parameters. Due to limitations of electrical components such as DAC, the binary electrical signals that drive the in-phase (I) and quadrature (Q) port of each IQ-MZM are generated by the unique DAC, using data and *data* for X and Y polarization separately. In this way, the BBC was implemented on both polarizations. At the receiver side, following the carrier extraction, a Gaussian filter with 28 GHz-bandwidth was applied to the signal to mitigate residual LO noise. System performance has been evaluated for the transmission of a 28 Gbaud-coded 16_QAM, using a block length of 4 on both polarizations. The simulations were performed for different optical signal-to-noise ratios (OSNRs), and the results of the obtained BER are illustrated in **Figure 10**, together with the experimental results. A negligible OSNR penalty was obtained utilizing BBC = 4 bits. **Figure 7** indicates the obtained 16-QAM constellations at BBC = 4 for both X and Y polarizations along with BER results, at OSNR = 18 dB and OSNR = 28 dB. As can be noticed from **Figures 6** and **7**, system performance is not affected by coding one or two polarizations, even if that yields a 25% rate reduction over a single polarization.

3.3 Experimental Validation

The experimental setup used for validation of the proposed SHCDT system is shown in **Figure 8**. It comprises two main blocks: transmitter (TX) and receiver (RX). At the transmitter side, the light source, a tunable external cavity laser (ECL, 14 dBm, 1550 nm), is split over two orthogonal polarizations, each one phase and amplitude modulated by IQ modulators and then recombined. Providing two orthogonal polarizations, CW is split over a 10:90 polarization-maintaining optical splitter (PM-splitter). While the 10% CW is launched into the first IQ-MZM, the 90% is split again through another 10:90 PM-splitter, providing the LO (90%) and fed to the second IQ-MZM (10%) to provide the X-polarization. After each IQ-MZM, an erbium-doped fiber amplifier (EDFA) is placed to compensate for modulation losses. The IQ modulators are driven by a two-channel, 6-bit, 100-GS/s DAC *via* two linear driver amplifiers. The DAC board has a 3-dB electrical bandwidth of 35 GHz. The DAC waveforms are preprocessed using offline DSP, including bit-to-symbol mapping and BBC. Consequently, both IQ-MZMs received the same information signal (PRBS11, data, and *data*) and the same modulation pattern (28 Gbaud, coded 16-QAM). Proper signal coding is applied (Nb = 4 bits) so that the modulated power around the DC is negligible. The output power of each IQ-MZM is set to be −2.5 dBm. The 11.5-dBm unmodulated carrier is coupled to the X-polarization coded 16-QAM through a 3-dB polarization-maintaining optical coupler. Exploiting a polarization beam combiner (PBC), the

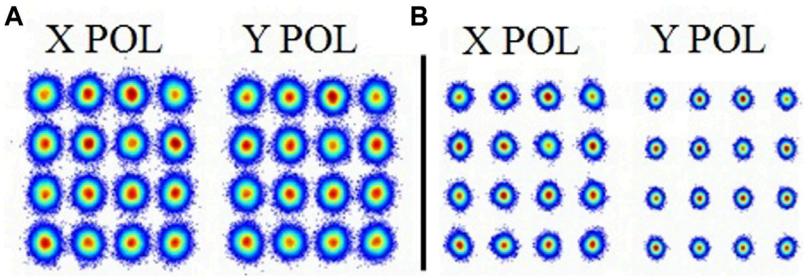

FIGURE 7 | Obtained constellations of 16-QAM (28 Gbaud) simulation, when both X and Y polarizations are coded (BBC length =4 bits), at different OSNRs. **(A)** Corresponding BER at OSNR = 18 dB is X-pol BER = 8.4589e-04, Y-pol BER = 8.5666e-04. **(B)** Corresponding BER at OSNR = 28 dB is X-pol BER =0.00, Y-pol BER = 0.00.

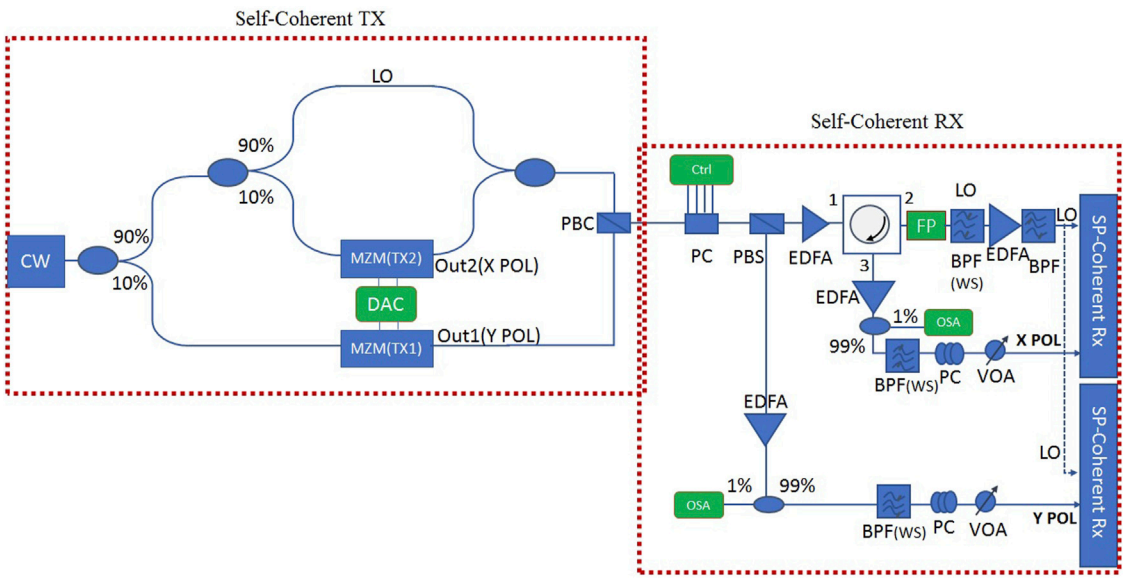

FIGURE 8 | Experimental setup for SHCDT evaluation in terms of BER measurement. The setup comprises two main parts: Self-coherent Tx and Self-coherent Rx. At the Tx side, LO, local oscillator (unmodulated carrier); MZM, IQ Mach–Zehnder modulator; PBC, polarization beam combiner. At the Rx side, PC, polarization controller; PBS, polarization beam splitter; EDFA, erbium-doped fiber amplifier; FP, Fabry–Perot filter; BPF, optical bandpass filter; WS, a wave shaper that is used as a tunable bandpass filter; VOA, variable optical attenuator; OSA, optical spectrum analyzer.

Y-polarization is recombined with the X-polarization that carried the LO.

At the receiver side, a tunable filter is required to extract the unmodulated carrier. Before the filter, a polarization controller aligns the input signal polarization state to the main propagation mode of the filter. In our setup, polarization is manually adjusted using a 4-channel polarization controller, where each polarization control axis is controlled by setting the input voltage of each channel. Following the polarization controller, a polarization beam splitter (PBS) is utilized to separate the transmitted orthogonal polarizations. The separated polarization states are amplified through EDFAs individually. Afterward, the Y-polarization is sent into the receiver and X-polarization to the carrier extractor. In our experimental setup, the carrier extractor consists of a Fabry–Perot (FP) filter, whose free spectral range (FSR) is ~1 nm and a bandwidth measured of ~900 MHz, followed by an optical circulator. The FP transfer function in reflection is a notch filter (band-stop). The Fabry–Perot filter and a circulator were used to separate the signal and LO. The extracted carrier (filter output) and the reflected signal (at port 3 of the circulator) were sent, individually, through the preamplifier (pre-amp) EDFA to the receiver. The pre-amp EDFA is used to compensate for FP loss. An optical bandpass filter was used after each pre-amp to reduce the amplifier noise. **Figure 9** indicates the signal spectrum at each stage, measured *via* a high-resolution optical spectrum analyzer.

In the interest of emulating a single-polarization receiver, one polarization at each time is sent to the receiver to mix with the extracted LO. To remove the residual signal on the extracted carrier, a wave shaper was used as a tunable bandpass filter with

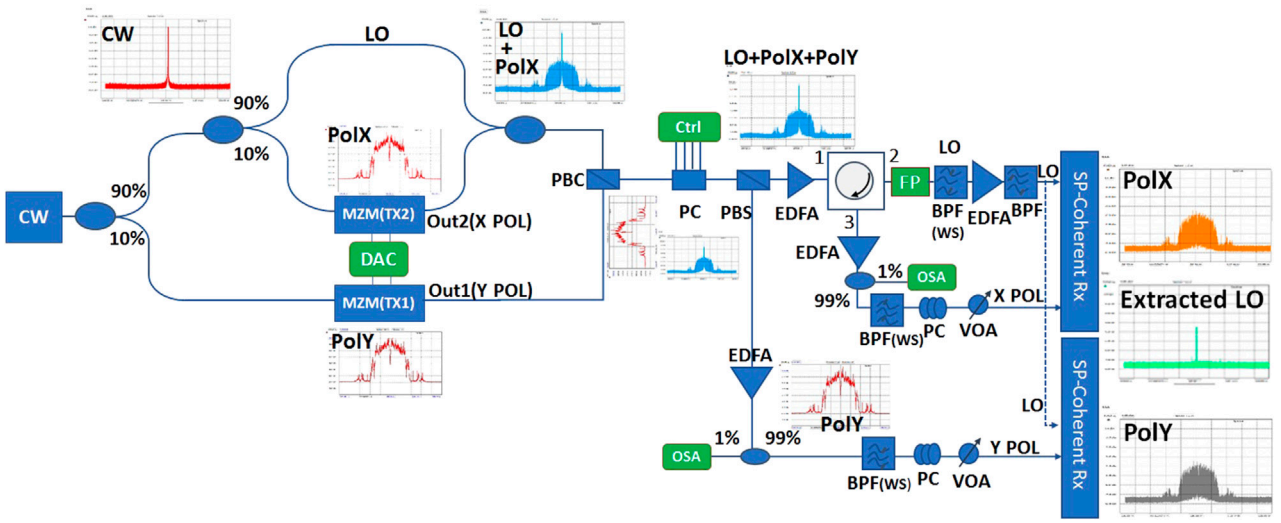

FIGURE 9 | Experimental configuration for SHCDT evaluation (as shown in Fig.9) along with the signal spectrum at each stage from generating at Tx to detecting at Rx. At the receiver side, both polarizations of the signal and the extracted LO are shown. Signal and LO spectrum measured *via* a high-resolution optical spectrum analyzer. PolX, reflected signal using FP; Extracted LO, extracted LO using FP; PoLY, signal with the Y polarization separated from X polarization at the PBS.

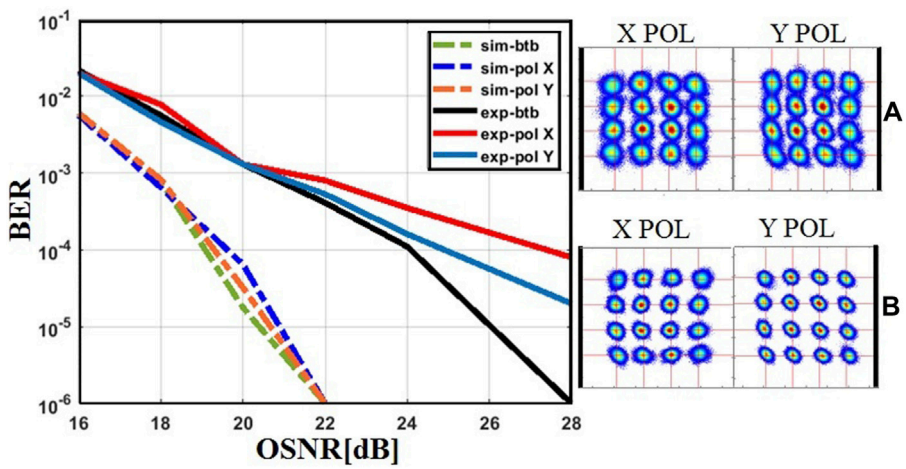

FIGURE 10 | Experimental BER measurements (28 Gbaud dual-polarization 16QAM) as a function of the received OSNR, utilizing a 900-MHz optical filter (FP) for local oscillation extraction along with simulation results. Both X and Y polarization are coded. **(A)** Received constellation at OSNR 18 dB with the corresponding BER of X-pol BER = 6.1055e-3, Y-pol BER = 4.1753e-3, and **(B)** received constellation at OSNR 28 dB with the corresponding BER of X-pol BER = 8.7078e-5, Y-pol BER = 2.9026e-5.

a narrow bandwidth and placed before the pre-amp EDFA. The received signal (single-polarization) was mixed with the extracted LO through a 90° optical hybrid, whose outputs were sent to four couples of balanced photodiodes. The four obtained signals were digitally processed for recovering the data through a 23-GHz 50 GSa/s real-time digital sampling oscilloscope. To optimize the performance, a narrow bandwidth Gaussian filter (order 4) with DSP is exploited as a bandstop filter to remove the residual LO on X-polarization followed by a Gaussian filter with 28 GHz bandwidth to mitigate the residual LO noise on X-polarization. Using a fine, narrow bandwidth filter for extracting the carrier avoids using the bandstop filter on DSP. The offline DSP at the receiver comprises optical front-end corrections, resampling to two samples per symbol, training-aided, and equalization. In this system, carrier-frequency offset compensation and dispersion compensation are unneeded, providing reduced DSP complexity. The bit-error-rate (BER) measurements have been evaluated as a function of the OSNR at the receiver individually for each polarization. As a first measure, we

evaluated the impact of BBC in a back-to-back configuration. The results showed no significant penalty introduced by the BBC filter as theoretically predicted. **Figure 10** illustrates the BER measurements as a function of the received OSNR in addition to the simulated one for both polarizations. This figure indicates the results for the back-to-back performance and transmission using BBC = 4 bits. An implementation penalty of approximately 4 dB is obtained at a BER of 10^{-4}. Moreover, a penalty of about 6 dB is demonstrated for X-polarization. As it can be noticed, in **Figure 10**, despite the filtering and carrier extraction of the X-polarization, there is no significant OSNR difference between the X and Y-polarization at a BER of 10^{-3}. The received 16-QAM constellations at OSNR = 18 dB and OSNR = 28 dB, for both X and Y polarizations, are also shown in **Figure 10**.

4 DISCUSSION

We proposed a self-coherent transmission detection (SHCDT) system suitable for high-capacity 5G short-reach communication. While the standard coherent transmission is carrier-suppressed, in the proposed system at the Tx, part of the CW light is sent together with the modulated signal over one of the two polarizations. A tunable optical filter extracts the optical carrier. The filter could be cost-effectively realized in silicon photonics. This CW light can be used as a local oscillator, avoiding in principle the need for polarization recovery, frequency offset compensation, and phase noise on the Rx. Before the filter, a polarization controller aligns the input signal polarization with the main propagation mode of the filter. Both the polarization controller and notch filter share the same control circuit. The control circuit rotates the signal polarization in the polarization controller until it matches the main propagation mode of the filter and adjusts the filter central frequency until the optical carrier power at the output of the filter is maximized. At the transmitter, signal encoding (BBC) is adopted with a cutoff frequency equal or higher than the bandwidth of the filter used for carrier extraction. In practice, polarization controllers are necessary if the Rx is based on polarization-sensitive components, such as silicon photonics. Phase rotations anyway occur due to differences in the optical path length of the CW light and signal. The proposed self-coherent system mitigates the phase noise transfer from the local oscillator to the received signal without requiring the use of expensive narrow-linewidth lasers. The proposed SHCDT system assures reducing the complexity, cost, and power consumption of the DSP. Low-cost solutions are enabled by photonic integration for polarization rotation, polarization splitting, and optical filtering. DSP complexity can be drastically reduced by utilizing the proposed techniques, making it an attractive solution for short-reach communications. In this research work, we carried out modeling, simulation, and experimental validation of SHCDT. We have investigated the system performance through simulation and experimental validation. We have shown the feasibility of carrier extraction by a tunable narrow bandwidth optical filter (Fabry–Perot filter) and coding technique (BBC). The impact of code efficiency on signal performance has been considered. We carried out a successful detection of the coded signal using the extracted carrier. The BER measurements have been evaluated as a function of the OSNR. The obtained results demonstrated negligible penalty on both polarizations.

DATA AVAILABILITY STATEMENT

The raw data supporting the conclusion of this article will be made available by the authors, without undue reservation.

AUTHOR CONTRIBUTIONS

PN designed and performed the experiments, performed the simulations, analyzed the results, and wrote the manuscript. MI characterized the FP filter and performed the experiments. FC provided vendor specifications. LP conceived and developed the concept, designed simulations, and reviewed the results and the manuscript.

REFERENCES

Adhikari, S., Jansen, S. L., Alfiad, M., Inan, B., Sleiffer, V. A. J. M., Lobato, A., et al. (20112011). Self- Coherent Optical OFDM: An Interesting Alternative to Direct or Coherent Detection. *ICTON* 1, 4. doi:10.1109/ICTON.2011.5971099

Alimi, I., Patel, R., Silva, N., Sun, C., Ji, H., Shieh, W., et al. (2021). A Review of Self-Coherent Optical Transceivers: Fundamental Issues, Recent Advances, and Research Directions. *Appl. Sci.* 11, 7554. doi:10.3390/app11167554

Cavers, J. K., and Marchetto, R. F. (1992). A New Coding Technique for Spectral Shaping of Data. *IEEE Trans. Commun.* 40 (9), 1418–1422. doi:10.1109/26.163561

Che, D., Li, A., Chen, X., Hu, Q., Wang, Y., and Shieh, W. (2014). Stokes Vector Direct Detection for Short-Reach Optical Communication. *Opt. Lett.* 39, 3110. doi:10.1364/OL.39.003110

Che, D., and Shieh, W. (2016). Polarization Demultiplexing for Stokes Vector Direct Detection. *J. Lightwave Technol.* 34, 754–760. doi:10.1109/JLT.2015.2511881

Chen, X., Che, D., Li, A., He, J., and Shieh, W. (2014). "102.4-Gb/s Single-Polarization Direct-Detection Reception Using Signal Carrier Interleaved Optical OFDM," in Proceedings of the OFC 2014, San Francisco, CA, USA, March 2014. doi:10.1364/OFC.2014.Tu3G.7

Chen, X., Che, D., Li, A., He, J., and Shieh, W. (2013). Signal-carrier Interleaved Optical OFDM for Direct Detection Optical Communication. *Opt. Express* 21, 32501. doi:10.1364/OE.21.032501

Greenstein, L. J. (1974). Spectrum of a Binary Signal Block Coded for DC Suppression. *Bell Syst. Tech. J.* 531103 (6)–1126. doi:10.1002/j.1538-7305.1974.tb02783.x

Imran, M., Goki, P. N., Potì, L., and Cavaliere, F. (2021). "Self-Homodyne Coherent Transmission for High-Speed Radio Access Networks (RAN) Employing Automatically Controlled Carrier Extractor," in Proceedings of the Photonics in switching and computing 2021, Virtual Event Canada, September 2021. doi:10.1364/PSC.2021.W3A.4

ITU (2019). *ITU-T, G.698.2: Amplified Multichannel Dense Wavelength Division Multiplexing Applications with Single Channel Optical Interfaces,*

Recommendation G.698.2. Available at: https://www.itu.int/rec/T-REC-G.698.2/en.

ITU (2020). *ITU-T, G.8300: Characteristics of Transport Networks to Support IMT-2020/5G, Std*. Available at: https://www.itu.int/rec/T-REC-G.8300-202005-I.

Morsy-Osman, M., and Plant, D. V. (2018). "A Comparative Study of Technology Options for Next Generation Intra- and Inter-datacenter Interconnects," in Proceedings of the 2018 Optical Fiber Communications Conference and Exposition (OFC), San Diego, CA, USA, March 2013. doi:10.1364/ofc.2018.w4e.1

Sacher, W. D., Barwicz, T., Taylor, B. J. F., and Poon, J. K. S. (2014). Polarization Rotator-Splitters in Standard Active Silicon Photonics Platforms. *Opt. Express* 22, 3777. doi:10.1364/OE.22.003777

Sowailem, M. Y. S., Morsy-Osman, M., Liboiron-Ladouceur, O., and Plant, D. V. (2016). "A Self-Coherent System for Short Reach Applications," in Proceedings of the 2016 Photonics North (PN), Quebec City, QC, Canada, May 2016. doi:10.1109/PN.2016.7537903

Velha, P., Sorianello, V., Preite, M. V., De Angelis, G., Cassese, T., Bianchi, A., et al. (2016). Wide-band Polarization Controller for Si Photonic Integrated Circuits. *Opt. Lett.* 41, 5656–5659. doi:10.1364/OL.41.005656

Conflict of Interest: Author FC is employed by Ericsson Italy.

The remaining authors declare that the research was conducted in the absence of any commercial or financial relationships that could be construed as a potential conflict of interest.